Effect of Deformation-Induced Martensite on the Fatigue Behavior of Metastable Austenitic Stainless Steels

H.-J. Christ,[1] *U. Krupp*[2]; *C. Mueller-Bollenhagen*[1]; *I. Roth*[1]; *M. Zimmermann*[1]
[1] *Universität Siegen, Siegen, Germany;*
[2] *Fachhochschule Osnabrueck, Osnabrueck, Germany;*
E-mail: Hans-Juergen.Christ@uni-siegen.de

1 Introduction

Metastable austenitic stainless steels can undergo a diffusionless phase transformation from austenite to martensite by deep cooling or plastic deformation under monotonic and cyclic loading. The fcc austenite transforms to the bcc α'-martensite or to the hcp ε-martensite phase [1]. It is well known that the α'-martensite can be used to modify the monotonic strength properties and that this transformation can also be beneficial for the LCF properties [2]. Investigations about the influence of martensite formation on short crack initiation and growth are very rare. Only in publications by Stolarz [3] information regarding the interaction between microstructure, plastic deformation induced martensite and short crack propagation can be found. However the design and production of cyclically loaded parts made of metastable stainless steel demands a substantial understanding of the correlation between fatigue life, martensitic transformation and damage mechanisms. This study focuses on these aspects and presents recent results with regard to in-situ-fatigue testing and fatigue strength derived from load increase-tests.

2 Experimental Details

Two AISI 304 austenitic stainless steels of different charges and microstructures were tested. Material I was tested in the as-received condition of 2 mm thickness using flat specimens. Material II was delivered as rods with 25.5 mm diameter and solution annealed before testing. Various sample geometries were manufactured from this batch. The chemical compositions of both charges are given in Table 1.

Tab. 1. Chemical composition.

Charge	Shape	Alloy	Fe	C	Cr	Ni	Si	Mn	Cu	Mo
I	sheet	AISI 304	Base	0.024	18.3	8.11	0.43	1.43	0.14	0.04
II	rod	AISI 304	Base	0.03	18.1	8.75	0.62	1.85	0.54	0.37

Flat tensile and fatigue specimens with a thickness of 2 mm were manufactured from the sheet material. Tensile tests at different strain rates and ambient temperatures were executed by means of a hydraulic testing machine (Schenck) equipped with a liquid nitrogen-cooled chamber. Temperature and martensite volume fraction were measured in-situ for all tensile tests. K-type thermocouples were taped on the tensile specimens for temperature measurements. The actual volume fraction of α'-martensite was measured applying a magneto-inductive measuring device (Fischer feritscope). By comparing the results of X-ray diffraction phase analysis with feritscope measurements, the feritscope was found to underestimate the martensite content. For the quantitative X-ray diffraction phase analysis the method reported in [4] was used. The correlation of feritscope and X-ray measurements gave a linear relationship. A factor of 1.58 was determined as appropriate to convert all feritscope readings into true volume fraction values of martensite.

Fatigue tests were carried out by means of a resonance pulsating test system (Rumul) at frequencies of about 90 Hz with a stress ratio of R = -1. All fatigue specimens were mechanically polished. In order to monitor the energy release caused by cyclic plastic deformation, temperature was measured with three spot-welded thermocouples as described in [5], one in the middle of the specimen (T_1) and two at both sides of the cut-out (T_2, T_3). A ΔT value was calculated using the equation

$$\Delta T = T_1 - 0.5\,(T_2 + T_3) \qquad \text{Eq. (1)}$$

to characterize the temperature increase in the gauge length relatively to the temperature of the solely elastically deforming grip sections. In this study specimens were not actively cooled and first experiments with cooled specimens showed that the following results are only valid for fatigue tests without cooling. The strong influence of the temperature of the specimens on the fatigue behavior is due to the sensitivity of the martensitic transformation to temperature.

Short crack growth experiments were carried out on cylindrical shallow notched specimens [6] in a Schenck S56 servohydraulic testing system and on flat specimens in a newly developed miniature testing system for in situ use in a scanning electron microscope (SEM) [7]. Before machining the rods were solution annealed for 1 h at 1050 °C resulting in a homogeneous microstructure with an average grain size of 54 µm and a minor content of delta ferrite. The tests were also executed at a load ratio of R = -1 and a frequency of 5 Hz under load control in the classical range of the fatigue limit ($\Delta\sigma/2$ = 230 MPa). In order to keep the temperature constant at room temperature, an air cooling was used. For the examination of the specimens a Philips XL30 LaB_6 SEM was used equipped with an automated electron back-scattered diffraction (EBSD) system (TSL OIM™) for phase analysis and crystal orientation measurement. For this purpose both kinds of specimens were electrochemically polished in order to achieve a smooth and deformation free surface.

3. Results and Discussion

3.1 Martensite formation under monotonic and cyclic loading

Stress vs. strain and martensite vs. strain curves for tensile tests of material I at different ambient temperatures are given in Figure 1. The tests were performed at a strain rate of 0.005 1/s leading to an increase in the temperature of the specimens and therefore to non-isothermal test conditions. The change in temperature was measured and all measured data was used to determine the constants of several material models proposed in literature to predict the martensite content. Most models were able to predict the martensite content in good agreement with experimental data for the non-isothermal experiments above 0 °C. Below 0 °C the martensite vs. strain curves change from a more parabolic to a strong sigmoidal shape (Figure 1), an effect which could not be reproduced properly by the models.

In Figure 1, the strong influence of the formation of martensite on the stress strain curves becomes obvious. With decreasing test temperature the amount of martensite formation increases and leads to a strong increase in tensile strength. From 23 °C to -40 °C the tensile strength is raised by about 40%. The ductility of the material was evaluated on the basis of the elongation at fracture. An optimum ductility can be seen at 10 °C in Figure 1 caused by the formation of a specific martensite content. Hence, it is evident that material properties under monotonic load can be controlled and enhanced by setting up specific contents of α'-martensite.

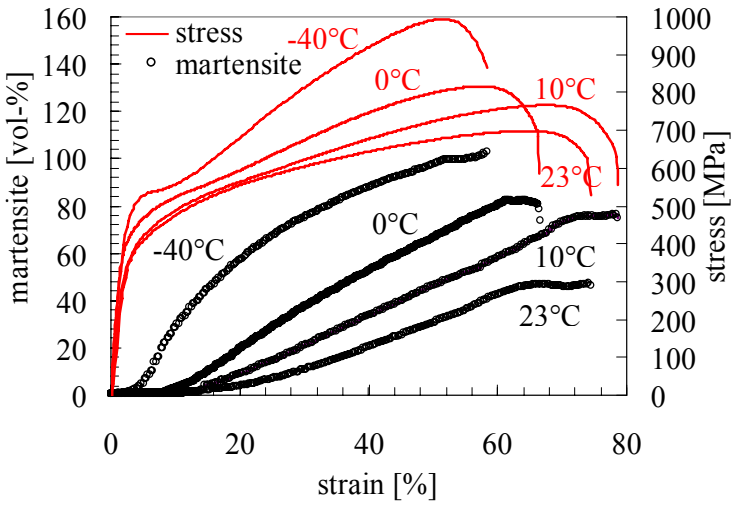

Fig. 1. Formation of martensite at different ambient temperatures during tensile deformation.

The martensite is not formed homogeneously across the cross-section of the specimens. Figure 2 shows color-etched micrographs of two tensile test specimens, one after 10% elongation (a) and one after 40% elongation (b). The dark areas are martensitic. Both micrographs illustrate the preferred transformation of martensite in horizontal lines most likely caused by micro-segregations. The thin dark needles in Figure 2 are presumably ε-martensite, what is confirmed by the little amount of α'-martensite measured in this state (0.95 vol.-%). The needles are mostly tilted 45° to the loading direction. Where ε-martensite needles intersect, blocks of α'-martensite are formed (white circles in Figure 2a). In the initial state of deformation the formation of ε-martensite is apparently predominant. For 40% of elongation mostly α'-martensite can be found, primarily in the center of the cross section of the specimen.

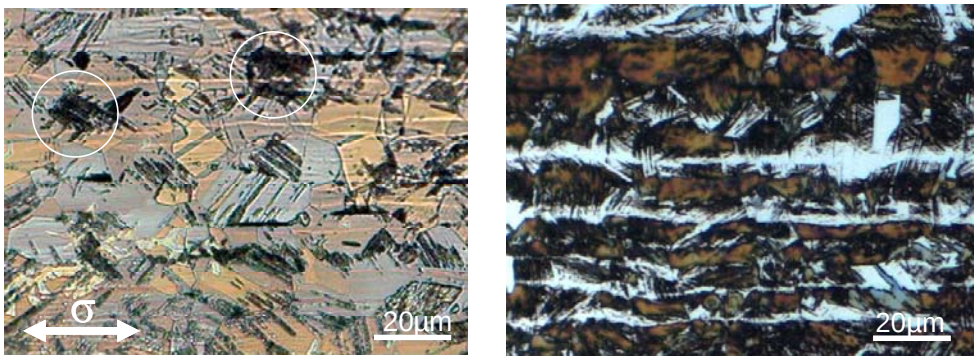

a) b)

Fig. 2. Micrographs of tensile test specimens after 10% (a) and 40% elongation (b).

It is well known that AISI 304 can also undergo a martensitic transformation under cyclic loading conditions [e.g. 1, 8]. Figure 3 shows the increase in thee α'-martensite fraction with increasing number of cycles at different temperatures. Similar dependencies and effects of martensite formation were observed as in the tensile tests. Martensite fraction generally increases with increasing number of cycles and therefore increasing cumulative plastic strain. The tests represented in Figure 3 were carried out at a constant total strain amplitude $\Delta\varepsilon/2$ of 0.5% using three different temperatures. It is clearly seen that the amount of martensite strongly increases with decreasing temperature. Martensite evidently leads to cyclic hardening at -100 °C and -50 °C and hence increases the stress amplitude. At 22 °C the amount of martensite measurable is below 5 vol.-%.

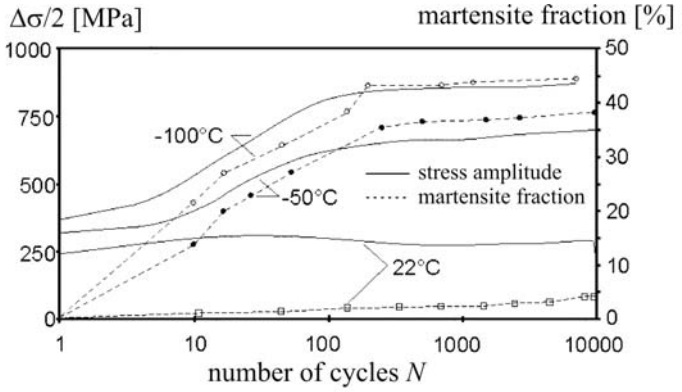

Fig. 3. Cyclic deformation and formation of martensite at different temperatures [1].

Since the material properties under monotonic load as well as fatigue properties in the LCF regime [1] are strongly influenced by the content of martensite such an influence was also assumed for the fatigue limit. In [9,10] it is suggested to use load-increase tests along with high resolution measurements of the temperature of the specimens for estimating the fatigue limit. Under these testing conditions, the fatigue limit can be defined as the stress amplitude, where the temperature strongly increases and does not converge to a horizontal asymptote within one loading step anymore. Hence, load-increase tests were carried out in order to determine the fatigue limit at different contents of martensite established by monotonic predeformation. The load increase tests were started at a stress amplitude of 200 MPa. The stress amplitude was then raised stepwise in 5 MPa steps every 10^4 cycles. As a consequence of the low stress amplitudes applied and the temperatures of the specimens in the tests the martensitic volume fraction can be considered to be unaffected by cyclic loading.

To quantify the correlation of martensite fraction and fatigue limit by means of load increase-tests, specimens with different contents of martensite are needed. Therefore, specimens of material I were deformed up to a plastic engineering strain of 15% at different temperatures below room temperature leading to different contents of martensite. Subsequently specimens were prepared as described in paragraph 2.

In Figure 4 the cyclic stress-strain behavior in load-increase tests of four different specimens with different martensite contents are shown together with the results of a load-increase test of a predeformed specimen. If the fatigue limit is estimated in the manner mentioned before, Figure 4 indicates clearly that the undeformed specimen in the pure austenitic condition shows the lowest fatigue limit. The specimen with a martensite content of 1.6% shows a much higher fatigue limit due to work hardening and seemingly the small amount of martensite. For the 30% specimen the fatigue limit is again significantly increased. However, further increase in martensite content lowers the fatigue limit again.

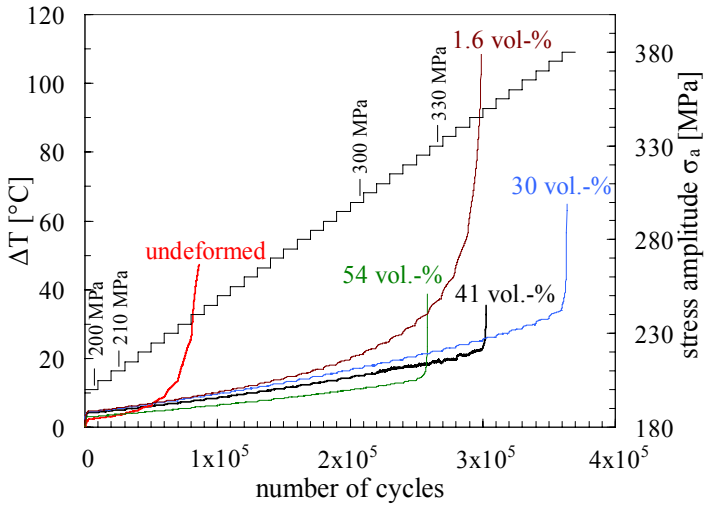

Fig. 4. Cyclic behaviour of specimens in load-increase tests at different martensite contents.

The damage mechanism, which leads to the strong dependence of the fatigue limit on the martensite content, will be further investigated during the continuation of this study. A most likely reason would be an increased notch sensitivity resulting from the degree of brittleness as a consequence of the martensite volume. First results for a more detailed understanding of the influence of martensite on the microstructural damage processes in the HCF regime will be discussed in chapter 3.2. As mentioned before, the tested specimens had small surface defects in the centre of the gauge length caused by the spot-welding of the thermocouples. For the three specimens with the highest martensite content this region was identified as origin of crack initiation.

3.2 Influence of microstructure and short crack growth on the martensite formation during cyclic loading

There is a general consensus that a deformation-induced formation of martensite does not occur during fatigue loading until thresholds of plastic strain amplitude ($\Delta\varepsilon_{pl}/2$) and cumulative plastic strain ($\Delta\varepsilon_{pl\text{-}cum}$) [11] have been reached. Although the threshold value of $\Delta\varepsilon_{pl}/2=0.3\%$ reported in [11] is not exceeded while testing at stress amplitudes near the fatigue limit, after some first 10^4 cycles a transformation can be observed in the scale of microstructure. The developed martensite appears as needles at activated slip systems, where the dislocation movement and, as a consequence, the local plastic deformation is high. A transformation from the fcc lattice to the bcc lattice is connected with a volume increase of 2-5% [12]. As a consequence the formation of the martensite needles leads to a surface roughening (Fig. 5 a) since the transformed volume expands forming extrusions on the specimen surface.

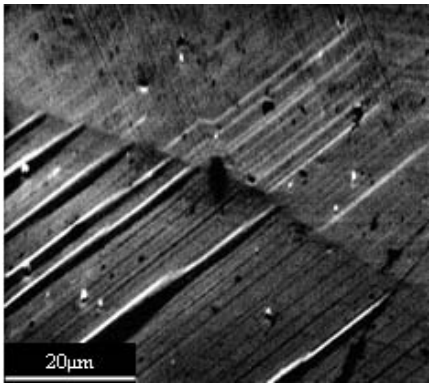

a)

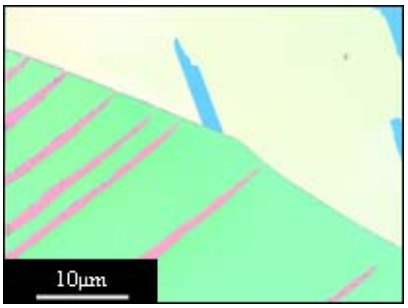

b)

Fig. 5. α′-martensite lamellae: a) SEM micrograph b) EBSD data: inverse pole figure map.

The EBSD data (Fig. 5 b) show that the crystal orientation of the martensite lamellae formed is uniform within the grains. Furthermore, the kind of martensite that is determined from the backscatter diffraction pattern is identified as bcc α′-martensite which is commonly found in 18/8 stainless steels [12, 13]. The existence of hdp ε-martensite could not be detected since it only appears during a transition period of the fcc to bcc transformation [13]. Presumably under the given conditions, the volume fraction of ε-martensite is not macroscopically detectable in contrast to the investigations in chapter 3.1 where ε-martensite could be detected in the bulk material.

In the plastic zone of short cracks, which initiate and grow at stress amplitudes in the high cycle fatigue (HCF) regime, a diffusionless phase transformation can be stated. This formation of α′-martensite appears with varying shape and crystallographic orientation (Fig. 6).

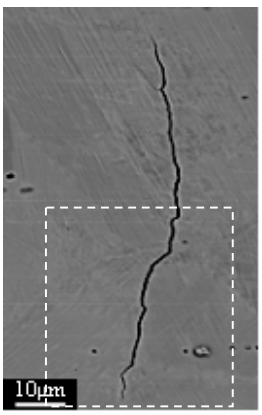

a)

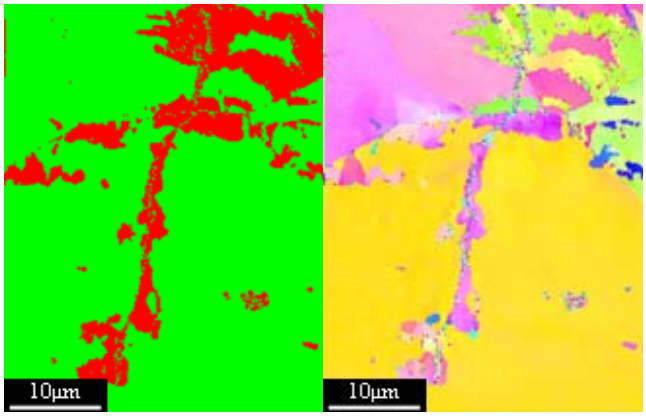

b) c)

Fig. 6. Martensitic transformation in the plastic zone of a propagating short crack: a) SEM micrograph, b) EBSD phase map (red: martensite, green: austenite), c) EBSD inverse pole figure map.

In order to establish a ground understanding of the damage mechanisms during cyclic deformation, the crystallographic relationship of the parent fcc austenite and the formed bcc martensite has to be determined. From the EBSD data, the orientation relationship between both crystallographic appearances of developed martensite, the lamellae at activated slip systems and the block-like martensite in the plastic zone of propagating short cracks are derived. It was found that {111} slip plane of austenite is parallel to {110} slip plane of martensite. Furthermore the slip directions <110> of martensite and <111> of austenite within the mentioned slip planes are parallel (Fig. 7). This correlation is characterized by the Kurdjumov-Sachs relationship (Eq. (2), Fig. 7) [13].

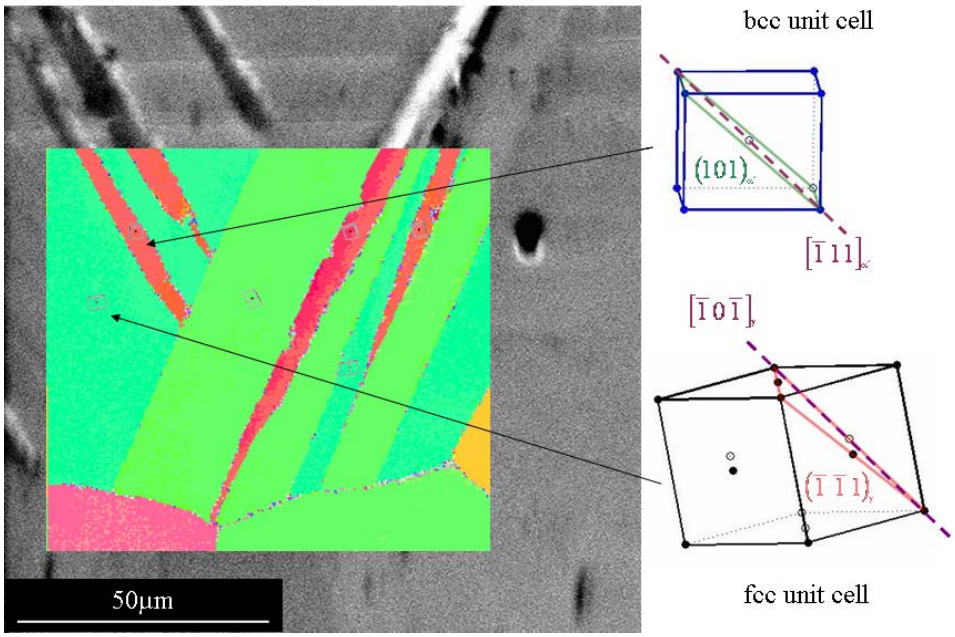

Fig. 7. Schematic representation of the crystallographic Kurdjumov-Sachs relation-ship [Eq. (2),13] between fcc lattice and bcc lattice of α´-martensite needles.

$$\left(\bar{1}\,1\,\bar{1}\right)_{\gamma} \text{ II } \left(101\right)_{\alpha'} \wedge \left[\bar{1}\,\bar{1}\,0\right]_{\gamma} \text{ II } \left[\bar{1}\,\bar{1}\,1\right]_{\alpha'} \qquad \text{Eq. (2)}$$

Ongoing investigations focus on how the crystallographic orientation of the martensite developed can be connected with a given load case and the structure of the initial austenite microstructure. In case of lamellae formed, the slip systems with the highest Schmid factor in austenite seem to be connected to the martensite that is formed according to the Kurdjumov-Sachs relationship. In the plastic zone of a growing short crack different slip systems may be activated. This could be an explanation for the block-like appearance of martensite. The correlation of these microstructural mechanisms and the fatigue limit requires future investigations.

4 Conclusions

The influence of deformation-induced martensite on the mechanical behaviour of AISI304L on a macroscopic and microscopic scale was surveyed. The results can be summarized as follows:

- The correlations between martensite content, loading parameters (strain, temperature), quasi-static strength properties and fatigue properties were shown and quantified. This knowledge may be helpful in an optimization of material properties of structural parts during forming processes.
- An optimum martensite content for the fatigue limit was determined to be approximately 30 vol.-%.
- During fatigue loading in the HCF regime, the formation of α´-martensite in local areas within microstructure was observed, although the global threshold value of plastic deformation has not been exceeded.
- α´-martensite develops as needles at activated slip systems and in the plastic zone of growing short cracks due to high local plastic deformation.
- The correlation of the crystallographic orientation of the fcc austenite and the bcc martensite lattice follows the Kurdjumov-Sachs relationship.

Acknowledgements

The authors wish to thank Deutsche Forschungsgemeinschaft (DFG) for financial support.

References

[1] U. Krupp, C. West, H.-J. Christ, Deformation-induced martensite formation during cyclic deformation of metastable austenitic steel: Influence of temperature and carbon content, Mater. Sci. Eng., A 481–482 (2008) 713-717

[2] H. J. Maier, B. Donth, M. Bayerlein, H. Mughrabi, B. Maier, M. Kesten, Optimierte Festigkeitssteigerung eines metastabilen austenitischen Stahls durch wechselverformungsinduzierte Martensitumwandlung bei tiefen Temperaturen, Z. Metallkd., 84 (1993), 820-826

[3] J. Stolarz, N. Baffie, T, Magnin, Fatigue short crack behaviour in metastable austenitic stainless steels with different grain sizes, Mater. Sci. Eng., A 319-321 (2001) 521-526

[4] A. K. De, D. C. Murdock, M. C. Mataya, J. G. Speer, D. K. Matlock, Quantitative measurement of deformation-induced martensite in 304 stainless steel by X-ray diffraction, Scripta Mater. 50 (2004) 1445-1449

[5] P. Starke, F. Walther, D. Eifler, PHYBAL—A new method for lifetime prediction based on strain, temperature and electrical measurements, Int. J. Fatigue 28 (9) (2006) 1028-1036

[6] O. Dueber, B. Künkler, U. Krupp, H.-J. Christ, C.-P. Fritzen, Experimental characterization and two-dimensional simulation of short-crack propagation in an austenitic-ferritic duplex steel, Int. J. Fatigue 28 (2006) 983-992

[7] I. Roth, M. Kübbeler, U. Krupp, H.-J. Christ, C.-P. Fritzen, In-situ analysis of small fatigue cracks in metastable austenitic steel and development of a mechanism-based modelling concept, Adv. Eng. Mater., submitted.

[8] M. Smaga, F. Walther, D. Eifler, Deformation-induced martensitic transformation in metastable austenitic steels, Mater. Sci. Eng., A 483–484 (2008) 394-397

[9] V. Wagner, B. Ebel-Wolf, F. Walther, D. Eifler, Very high cycle fatigue of railway wheel steels, in: J. E. Allison, J. W. Jones, J. M. Larsen, R. O. Ritchie (Eds.), Proc. of the 4. Int. Conf. on Very High Cycle Fatigue, TMS Publications, 2007, pp. 137-142

[10] D. Dengel, H. Harig, Estimation of the fatigue limit by progressively increasing load tests, Fatigue Fract. Eng. Mater., 3 (1980), 113-128

[11] M. Bayerlein, H.-J. Christ, H. Mughrabi, Plasticity-induced martensitic transformation during cyclic deformation of AISI304L stainless steel, Mater. Sci. Eng., A 114 (1989) L11-L16

[12] P. L. Mangonen Jr., G. Thomas, The martensite phase in 304 stainless steel, Metall. Trans. A 1 (1970) 1577-1586

[13] F. E. Fujita, On the lattice deformation in martensite transformation of steel, Metall. Trans. A 8A (1977) 1727-1736